

Article

Not peer-reviewed version

---

# Advancing Electric Load Forecasting: Leveraging Federated Learning for Distributed, Non-Stationary, and Discontinuous Time Series

---

[Lucas Richter](#)<sup>\*</sup>, Steve Lenk, Peter Bretschneider

Posted Date: 17 May 2024

doi: 10.20944/preprints202405.1157.v1

Keywords: Federated Learning; Load Forecasting; Non-Stationary And Discontinuous Time Series; Renewable Energy Community; Dynamic Portfolio



Preprints.org is a free multidiscipline platform providing preprint service that is dedicated to making early versions of research outputs permanently available and citable. Preprints posted at Preprints.org appear in Web of Science, Crossref, Google Scholar, Scilit, Europe PMC.

Copyright: This is an open access article distributed under the Creative Commons Attribution License which permits unrestricted use, distribution, and reproduction in any medium, provided the original work is properly cited.

Article

# Advancing Electric Load Forecasting: Leveraging Federated Learning for Distributed, Non-Stationary, and Discontinuous Time Series

Lucas Richter<sup>1</sup>, Steve Lenk<sup>1</sup> and Peter Bretschneider<sup>2</sup>

<sup>1</sup> Fraunhofer IOSB - Applied System Technology; Am Vogelherd 90, 98693 Ilmenau, Germany;

<sup>2</sup> TU Ilmenau - Energy Usage Optimization; Ehrenbergstraße 29, 98693 Ilmenau, Germany;

\* Correspondence: lucas.richter@iosb-ast.fraunhofer.de; Tel.: +49 3677 461146

**Abstract:** This paper addresses the evolving landscape of electricity markets in Europe, with a focus on the integration of Renewable Energy Communities as introduced by the Renewable Energy Directive 2018/2001. Residents within a postal code area are highly incentivized to join a community, which enables them to exchange energy among themselves at lower procurement costs. Thereby, energy management systems optimize the operation of respective energy systems, with electrical load forecasting playing a key role. Given that prosumers may switch between communities on a daily basis, electricity demands within these groups will vary, leading to data that is non-stationary, discontinuous as well as non-identical and independently distributed. To encounter this issue, we propose a sophisticated forecasting model that applies federated learning, using informations from various distributed communities to learn domain-invariant features. To achieve this, we initially utilize synthetic electrical load time series at district level and aggregate them to profiles of Renewable Energy Communities with dynamic portfolios. Subsequently, we develop a forecasting model that accounts for the composition of residents of a Renewable Energy Community, adapt data pre-processing in accordance with the time series process, and detail a federated learning algorithm that incorporates weight averaging and data sharing. Following the training of various experimental setups, we ultimately evaluate their effectiveness. The findings suggest that our proposed framework is capable of effectively forecast non-stationary and discontinuous time series and that it can be applied to new, unseen data through the integration of knowledge from multiple sources.

**Keywords:** Federated Learning; Load Forecasting; Non-Stationary And Discontinuous Time Series; Renewable Energy Community; Dynamic Portfolio

## 1. Introduction

### 1.1. Renewable Energy Directives

The industrial revolution brought about the automation of numerous work tasks, leading to enhanced productivity and better standards of living. However, this progress came with the adverse consequence of increased CO<sub>2</sub> emissions due to fossil fuel consumption, contributing to an increase in Earth's temperature of over 1K [1]. Looking ahead, Germany's energy infrastructure may confront various issues, particularly with the shift toward decentralized power generation. Policy changes at European and national levels have dismantled electricity grid monopolies, enabling consumers to choose their own power and gas suppliers in a competitive landscape. The fifth European energy package aims to align with the Paris Climate Agreement by advocating for the expansion of renewable energy and enhancing efficiency in industries such as manufacturing, transportation, and housing [2]. Investment incentives are essential to achieve these objectives, and to this end, the Renewable Energy Directive (RED II) defines Renewable Energy Communities (REC) (Definition 1) [3]. REC participants can share and utilize self-generated heat or electrical power at lower costs. Beyond regional growth, these initiatives allow for the optimization of local energy efficiency by coupling electricity, heating, and transport sectors [4].

**Definition 1** (Renewable Energy Community taken from [3]).

1. Consists of at least 50 natural persons
2. At least 75% of the shares are held by natural persons who are located within one postal area and a radius of 50 kilometers
3. No member possess more than 10% of the shares

### 1.2. Renewable Energy Management Systems

Regulatory and legislative developments are reshaping the dynamics of the electricity market, with emerging opportunities for district energy management systems (DEMS) - coming potentially with seventeen principal roles and an innovative IT framework in this sector [5]. Boundaries of districts are defined by either a local network transformer or a gas pressure regulator, setting them apart from neighboring districts, with each having its own unique spatial dimensions. These districts - whether located in urban, suburban, rural, or industrial settings, as well as those with mixed characteristics - have unique socio-economic and demographic features that influence their energy consumption [6,7]. Initiatives such as retrofitting buildings and modernizing heating systems can lead to lower energy consumptions. Leveraging smart demand-side management, flexible approaches in generating, consumption, and storing energy can diminish building heating demands by as much as 20% [8]. As we move towards sustainable energy supply, the orchestrated operation of buildings is gaining importance [7]. DEMS are instrumental in facilitating sector integration, minimizing electricity losses, enhancing supply reliability, and incorporating emergent technologies into the electrical grid [4]. They additionally have to control and optimize energy generation, consumption and storage resources - satisfying demands of specific balancing groups [9,10]. REC energy management systems (REC-EMS) surpass DEMS by taking on the responsibility of monitoring energy distribution and fostering synergies among various districts.

### 1.3. Use Case

The growing complexity of decentralized energy networks necessitates for advanced REC-EMS that facilitate automated data management across distributed systems, intelligently linking components within a REC to foster synergies and leverage flexibilities between RECs [7]. In addition to the rising use of heat pumps and electric vehicles, energy providers are obligated to provide customers with dynamic electricity pricing in accordance with EnWG (§41a) in Germany [11]. As storage systems engage with dynamic pricing, a variety of feedback mechanisms may arise, potentially resulting in electricity consumption that is sensitive to price changes [12]. To ensure the cost-effectiveness of REC-EMS, it is essential to develop REC energy consumption forecasting algorithms (REC-ECF) that are both scalable and transferable. With the energy market's liberalization allowing prosumers freely to select their energy provider on a daily basis [13], RECs possess a dynamic portfolio of their members, as depicted in Figure 1. These members represent either particular residents of a specific REC or various elements of the energy system such as electric vehicles and heat pumps. Given that each has distinct consumption patterns, the consequent time series data tend to be non-stationary (Definition 2) and exhibit discontinuities (Definition 3). Under these circumstances, a predictive model must account for the varied member composition and be calibrated for a range of RECs. The essential objective is to uncover cross-domain as well as domain-invariant patterns within a forecasting model that can handle various time series characteristics and enhance systems with time-sensitive variations.

**Definition 2** (Non-Stationarity, taken from [14]).

*A time series is considered stationary when its statistical characteristics remain consistent regardless of the observation time. In other words, the properties of a stationary time series do not change over time. On the contrary, if a time series exhibits trends or seasonality, it is considered non-stationary. The presence of trends or seasonality causes variations in the time series values at different points in time.*

**Definition 3** (Discontinuity).

*Discontinuous time series possess bounds in the sequence of observations.*

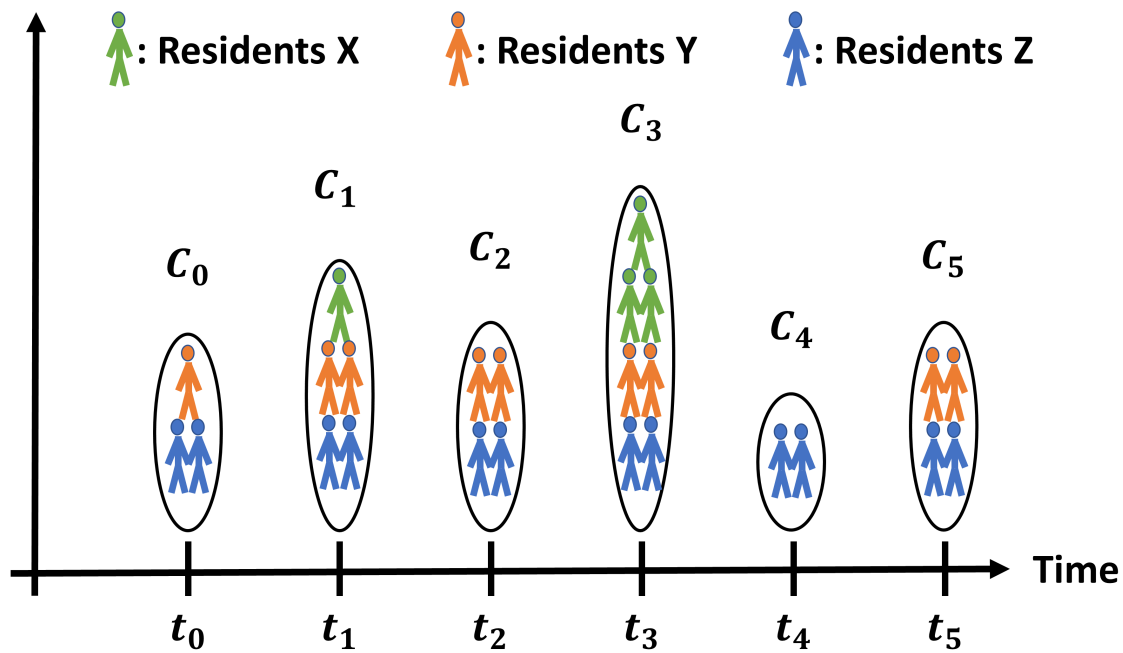


Figure 1. Time-variant portfolios  $C_0, C_1, C_2, C_3, C_4, C_5$  of RECs.

#### 1.4. Contributions

There is extensive research on electrical load forecasting, with many studies claiming to outperform other algorithms. On the contrary, reviews of numerous works on this subject often conclude that they are not truly comparable due to differences in the level of aggregation, the dataset used, the forecast model applied, the data preprocessing step, the temporal resolution, and the forecast horizon. Moreover, a standard benchmark model for time series forecasting is lacking, the process behind time series is frequently under-detailed, the problem concerning model weight divergence in a non-identical and independently distributed (non-iid) setting is only inadequately studied, issues such as non-stationarity and discontinuity are often ignored, and significant influences of the forecast execution time on forecast results is rarely considered [15]. With respect to the explainability and interpretability of machine learning models designed for time series forecasting, there is still a deficiency [16]. Investigations into the sensitivity to input features, uncertainties tied to conditionals, and the robustness to novel scenarios are still needed when utilizing machine learning (ML) models [17]. Recent studies on time series forecasting analyze various use cases by training models with highly stochastic and distributed household data using federated learning (FL) (Definition 4). These studies primarily focus on comparing strategies for averaging model weights and clustering data, with a one-step-ahead forecast horizon, to tackle challenges associated with non-iid data [18–23]. Given the aforementioned research gaps, we propose a time series forecasting framework that aggregates knowledge from multiple clients and is simultaneously capable of handling non-stationary, discontinuous, and non-iid data. Our work is structured as follows (Figure 2): (i) Analyze synthetic electrical load time series at the district scale, aggregate them to those of RECs with dynamic portfolios and prove non-stationarity, discontinuity and non-iid [15], (ii) describe data pre-processing concerning the time series process, the resulting time series forecasting model architecture, and federated learning strategies regarding non-iid data and model weight divergence, (iii) define experimental setups, and (iv) evaluate and discuss the results.

**Definition 4** (Federated Learning, inspired by [24,25]).

*Federated learning is a machine learning technique where a central model is trained across multiple devices holding local data, without exchanging it, thus preserving privacy and reducing data transfer. Local models' updates are aggregated to improve the central model.*

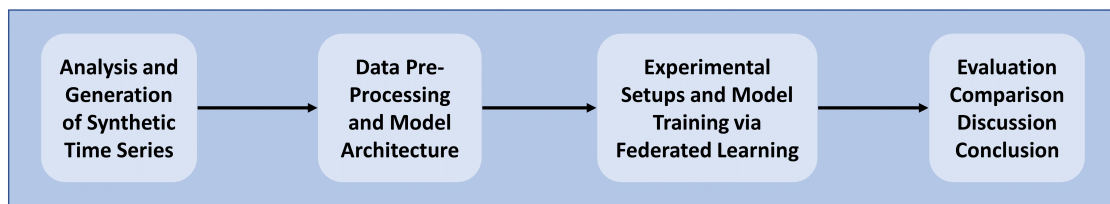


**Figure 2.** Based on the research objective, non-stationary as well as discontinuous time series of REC are firstly synthesized and subsequently validated for compliance with the required characteristics. Secondly, the process of electricity consumption time series, the equations related to data pre-processing, and the detailed description of the forecast model architecture are provided. With this in mind, the federated learning algorithm and research experiments are then presented. Following their execution, the results are shown and discussed in the final section to draw conclusions for future research.

## 2. Data

To address the research objective, to conduct various experiments, to evaluate results and lastly to discuss them (Section 1.4), a huge amount of REC time series is essential, ones that encompass necessary attributes such as non-stationarity (Definition 2), discontinuity (Definition 3), stochasticity (Definition 5), autoregression (Definition 6), seasonality (Definition 7), trend (Definition 8), periodicity (Definition 9) and non-iid on various clients. Figure 3 illustrates differences between these terms, where (a), (b), (c), (d), (f) and (g) are showing non-stationary characteristics (Definition 2). For simplicity, we assume that RECs are composed of various districts (Section 1.2). Since no real dataset fulfills these requirements, we firstly generate stationary as well as distinctive district electricity consumption time series (DECTS) based on different socio-economic factors (Section 2.1). Subsequently, we use these to construct RECs with dynamic portfolios, resulting in non-stationary and discontinuous time series (Section 2.2).

### Definition 5 (Stochasticity).

*The stochasticity of a time series refers to the inherent randomness or unpredictability in the data.*

### Definition 6 (Autoregression).

*Autoregression is a time series modeling technique where future values are predicted based on past values of the same series.*

### Definition 7 (Seasonality).

*Seasonality in time series is a long-term characteristic pattern that repeats at regular intervals (years).*

### Definition 8 (Trend).

*The trend of a time series represents a long-term linear or even non-linear time-dependency in the data, typically showing sustained increase or decrease over time.*

### Definition 9 (Periodicity).

*The periodicity of a time series refers to short-term, repetitive occurrences of specific patterns such as day of week or hour of day.*

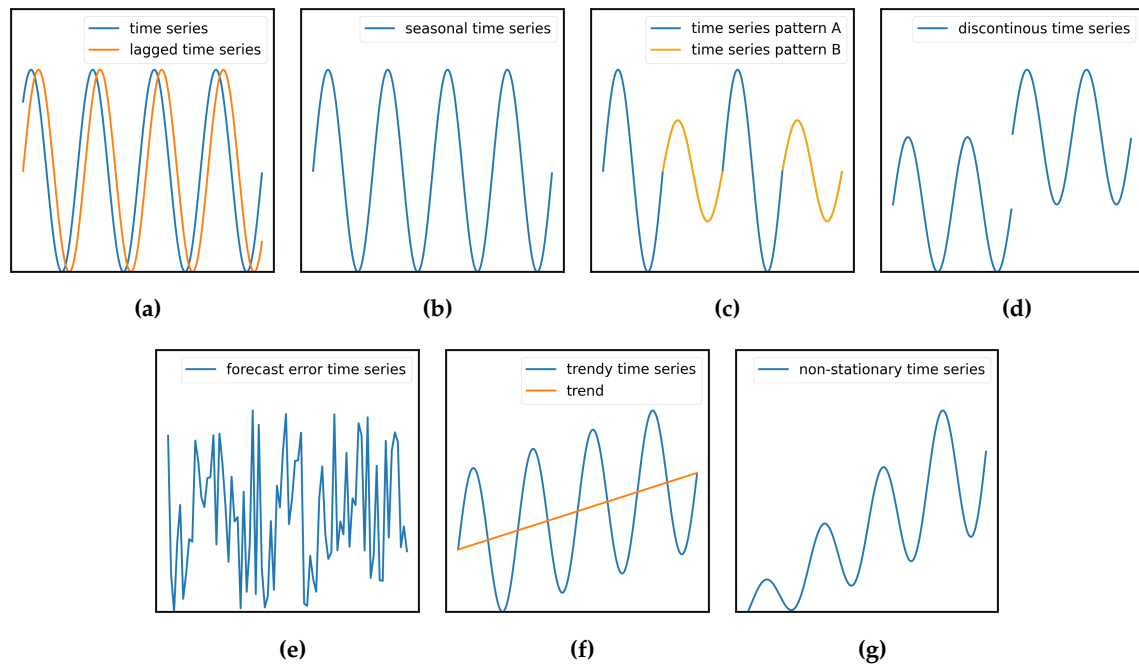


**Figure 3.** Different time series characteristics: (a) autoregression illustrated by showing a time series to its lagged version, (b) seasonal time series with recurrent patterns, (c) periodic time series with different recurrent patterns, (d) discontinuous time series with bounds in observations, (e) showing stochasticity referring to the time series forecast error, (f) seasonal time series with linear trend, (g) time series with linear and seasonal trend

### 2.1. Synthesis And Analysis Of Synthetic Electrical Load Time Series At District Scale

We utilize a public dataset that provides more than 5500 household electricity consumption time series with a 30-minute temporal resolution, classified into 18 different ACORN groups (Definition 10), to handle the huge amount of DECTS with diverse characteristics. Since these time series are highly stochastic, we proceed as introduced in [15]: (i) Clustering ACORN household electricity consumption time series, and transforming and scaling non-Gaussian distributed data, (ii) aggregating household data to the level of districts and extracting the time series process to ensure adequate sampling of training data, (iii) training a two-step probabilistic forecasting model to ensure both seasonal and short-term variations, and (iv) iteratively generate synthetic time series. This approach is applied in conjunction with weather data (temperature, relative humidity) of central Germany for the years 2018 and 2019. It results in a total of 55 distinct ACORN subgroups, each with specific time series characteristics influenced by socio-economic factors and household size. To gain a clearer understanding of the diversity of their characteristics, we firstly calculate a correlation matrix  $X_{cor}$  to obtain correlations between all ACORN subgroups. We then perform principal component analysis to reduce the dimensions to two and to illustrate it with a scatter plot (Figure 4). Since many ACORN subgroups possess similar electricity consumption characteristics, aggregating them to the level of a REC will not generate diverse time series. Therefore, we additionally apply K-means clustering with the number of clusters set to  $k = 10$ , extracting the ten most distinctive subgroups. The effect of this filtering method is demonstrated in Table 1, showing lower mean values and higher standard deviations of  $X_{cor}$  for the ten most distinctive subgroups, resulting in a higher diversity.

**Table 1.** Statistics of unfiltered and filtered datasets, with respect to DECTS of various ACORN subgroups, indicating higher diversity for the filtered case.

	$\mu(X_{cor})$	$\sigma(X_{cor})$
Unfiltered 55 ACORN subgroups	0.88	0.08
Filtered 10 ACORN subgroups	0.82	0.12

**Definition 10** (ACORN, taken from [26]).

ACORN is a segmentation tool which categorizes UK's population into demographic types.

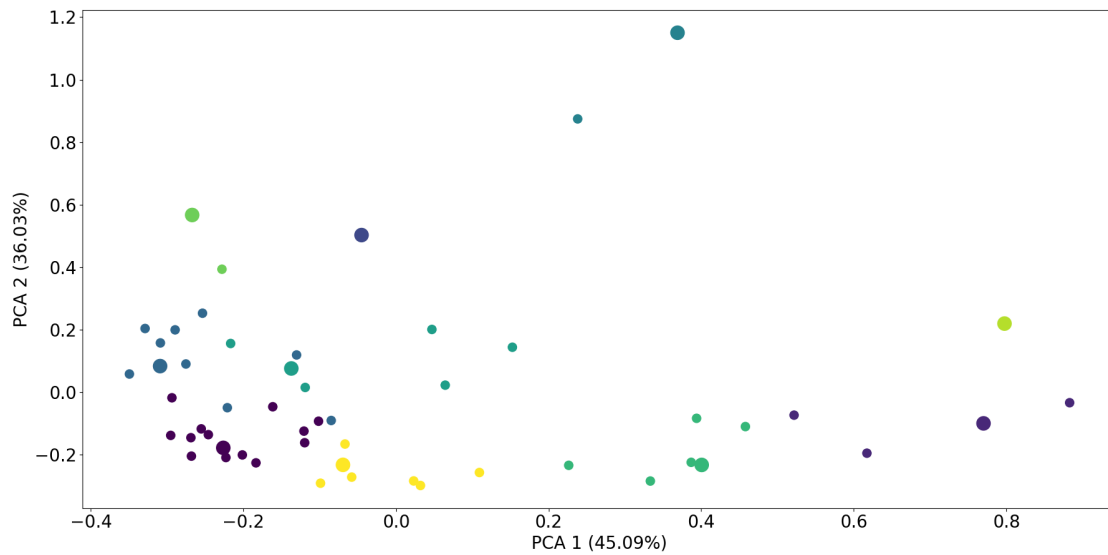


**Figure 4.** Illustrating two dimensional principal components of  $X_{cov}$ , clustered with K-means and number of clusters  $k = 10$ . Each color represents subgroups belonging to one cluster, while thick points depict the central subgroups within each cluster.

## 2.2. Generate Dynamic Portfolios Of Renewable Energy Communities

Besides the general definition of non-stationarity (Definition 2), there even exist more refined ones named cyclostationarity (Definition 11) [27]. Since synthetic REC time series (RECTS) should be constructed to satisfy a dynamic portfolio, they must not exhibit this characteristic. Keeping this in mind and given a set of 300 DECTS for each ACORN subgroup, we generate diverse RECTS from the ten most distinctive ones (Section 2.1) in respect of certain constraints (Algorithm 1):

1. No unique DECTS have to be used twice.
2. Each RECTS is composed of different DECTS in varying quantities  $N \in [0, 7]$ , depicting a time dependent residents composition vector  $\vec{r}_t$  (Eq. (1)) for each REC.
3. Since  $\max(N) = 7$  and only 300 DECTS exist for each ACORN subgroup, the quantity of RECTS is confined to 70.
4. Each REC is assigned both a random start and a random end  $\vec{r}_t$  with random various probabilities  $p \in [0.1, 0.2, 0.3, 0.4, 0.5, 0.6, 0.7, 0.8]$  that  $N_{i,t}$  is set to zero.
5. The residents composition of REC is linearly developed using start and end  $\vec{r}_t$ .
6. Every new day, one of ten ACORN subgroups is randomly chosen and either a new DECTS is added or an existing one is excluded, unless the linear development curve from start to end  $\vec{r}_t$  is undershot or exceeded by more than 1.

$$\vec{r}_t = [N_{1,t}, \dots, N_{10,t}] \quad (1)$$

where:

$N_{i,t}$  : Quantity of specific ACORN subgroup at time  $t$

$i$  : Index of specific ACORN subgroup,  $i \in [1, 10]$

$t$  : Index of time with a daily temporal resolution

**Definition 11** (Cyclostationarity, taken from [27]). A time series may exhibit both seasonality as well as periodicity and can still remain predictable, as these cyclical patterns repeat at regular intervals. Removing these two components will strongly lead to a stationary time series.

**Algorithm 1:** Generation of non-stationary and discontinuous RECTS

---

```

1 #Parameters:
2  $N \leq 7$  (Maximum number of DECTS from one specific ACORN subgroup within  $\vec{r}_t$ )
3  $k = 10$  (Number of distinctive ACORN subgroups used)
4  $L = 730$  (Number of days within each DECTS)
5
6 #Data:
7  $X = \{DECTS_{i,j}\}$   $X$  is the entire dataset of various DECTS
8 Index  $i \in [1, 10]$  depicts a specific ACORN subgroup
9 Index  $j \in [1, 300]$  depicts a unique DECTS
10
11 #Initialize residents composition vectors of RECs:
12 Randomly choose a probability  $p$  for indices to be zero from the set
    $[0.1, 0.2, 0.3, 0.4, 0.5, 0.6, 0.7, 0.8]$ 
13 for  $\vec{r}_{t=1}$  and  $\vec{r}_{t=L}$  do
14   | Generate random vector of length  $k$  within integer interval  $[0, N]$  and set values to zero
   |   using binomial distribution and  $p$ 
15
16 #Develop linear residents composition of RECs:
17  $grad = \left( \frac{\vec{r}_{t=L} - \vec{r}_{t=1}}{L} \right)$ 
18 for  $i \leftarrow 2$  to  $L$  by 1 do
19   |  $\vec{r}_{t=i} = int(\vec{r}_{t=i-1} \times grad)$ 
20
21 #Develop stochastic residents composition of RECs:
22 Replicate  $\vec{r}_t$  to  $\vec{s}_t$ 
23 for  $i \leftarrow 2$  to  $L - 1$  by 1 do
24   |  $\vec{s}_{t=i} = \vec{s}_{t=i-1}$ 
25   | Let  $idx$  be chosen randomly from vector  $[1, 2, 3, 4, 5, 6, 7, 8, 9, 10]$ 
26   | Sample one number  $z$  from a Gaussian distribution with  $\mu = 0$  and  $\sigma = 1$ 
27   | if  $z \leq 0$  then
28   |   |  $cnt_{idx} = \vec{s}_{t=i}[idx] - 1$ 
29   |   | if  $\vec{r}_{t=i}[idx] - cnt_{idx} > 1$  then
30   |   |   |  $pass$ 
31   |   | else
32   |   |   |  $\vec{s}_{t=i}[idx] = cnt_{idx}$ 
33   |   | else
34   |   |   |  $cnt_{idx} = \vec{s}_{t=i}[idx] + 1$ 
35   |   |   | if  $\vec{r}_{t=i}[idx] - cnt_{idx} < -1$  then
36   |   |   |   |  $pass$ 
37   |   |   | else
38   |   |   |   |  $\vec{s}_{t=i}[idx] = cnt_{idx}$ 
39
40 #Assign certain DECTS from an ACORN subgroup to a time-dependent REC membership
    $M_{t,i}$  based on  $\vec{r}_t$ . From one timestamp to the next, only one DECTS from a randomly
   selected ACORN subgroup may be added to or removed from  $M_{t,i}$ , e.g.,
    $M_{t=1,i} = \{\{1, 76, 276\}_{i=1}, \dots, \{25, 34, 101, 132, 189, 201, 222\}_{i=10}\}$ 
41
42 #Generate stochastic, non-stationary and discontinuous RECTS:
43 Initialize list  $X$  to which daily sequences will be appended
44 for  $i \leftarrow 1$  to  $L$  by 1 do
45   | Choose daily sequences with indices  $M_{t=i}$  from  $DECTS_{i,j}$ , aggregate them and append to
   |    $X$ 

```

---

### 2.3. Analyze Time Series Of Renewable Energy Communities

While Section 2.2 generates RECTS (examples of those can be found in Appendix B and Figure A1), we still have to test for required time series attributes. To address non-stationarity, we remove seasonality (week of the year), periodicity (day of the week, hour, minute), and even the long-term trend from the original time series by applying a Seasonal-Trend decomposition using LOESS of the Python statsmodels package. Subsequently, we apply the Augmented Dickey-Fuller (ADF) test on a representative RECTS, considering only timestamps at 12:00 (Figure 5). The Dickey-Fuller test is a statistical method for testing whether a time series is non-stationary and contains a unit root. The null hypothesis is that there is a unit root, suggesting that the time series has a stochastic trend. The ADF test considers extra lagged terms (we use  $maxlag = 7$  to account for an entire week) of the time series' first difference in the test regression to account for serial correlation. Since  $critical\ value > t - values$  at 1%, 5%, 10% confidence intervals, the null hypothesis can not be rejected, demonstrating non-stationarity of RECTS (Table 2, for all RECTS see Appendix A and Table A1).

**Table 2.** Test statistics of ADF check if RECTS is non-stationary.

critical value	pvalue	1%	5%	10%
-1.58	0.49	-3.44	-2.87	-2.57

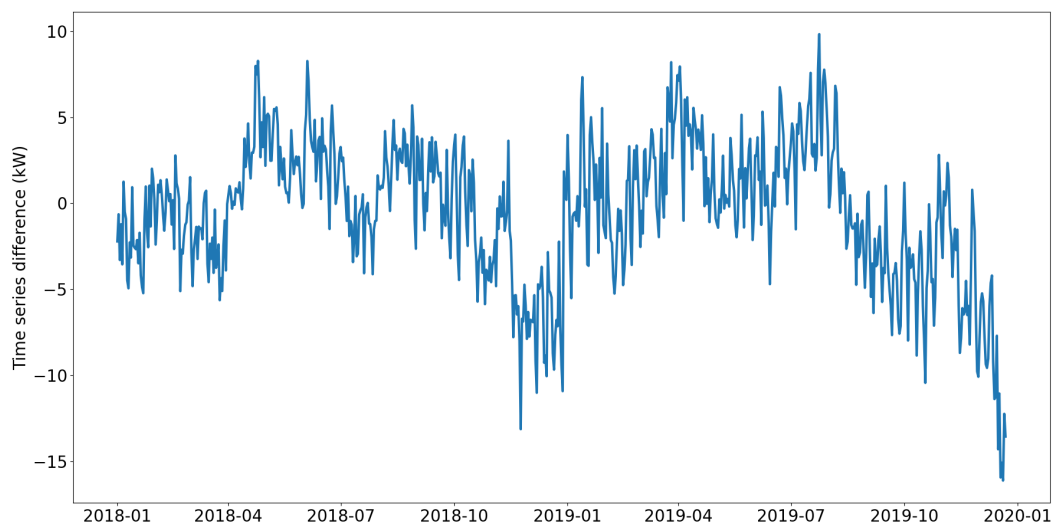


**Figure 5.** Resulting time series after removing seasonality, periodicity and trend at 12:00.

Discontinuity is often attributed to a change point, which indicates a transition from one state to another in the process generating the time series data. Various algorithms have been utilized to detect change points in data, including likelihood ratio, subspace model, probabilistic, kernel-based, graph-based and clustering methods [28]. In contrary, a boxplot is easy to use and give overview about data distribution, skewness and outliers [29]. In this, the box shows the interquartile range (IQR) which is the distance between the first (Q1) and third (Q3) quartiles. The whiskers extend from the box to the highest and lowest values within  $[Q1 - 1.5 \times IQR, Q3 + 1.5 \times IQR]$ . The line in the middle of the box represents the median or the second quartile (Q2) of the data. Points outside the whiskers represent outliers. To analyze discontinuity in RECTS, we firstly calculate mean daily sequences for each week of the year. Subsequently, we compute differential time series (time series minus its lagged version with shift of 1). Considering that all 70 RECTS have varying magnitudes, we normalize them by utilizing Eq. (2). Then, we use a boxplot to illustrate the distribution of all generated RECTS for each week of the year (Figure 6), showing a huge number of outliers and proving discontinuity in data.

$$x' = \frac{x}{\max(x)} \quad (2)$$

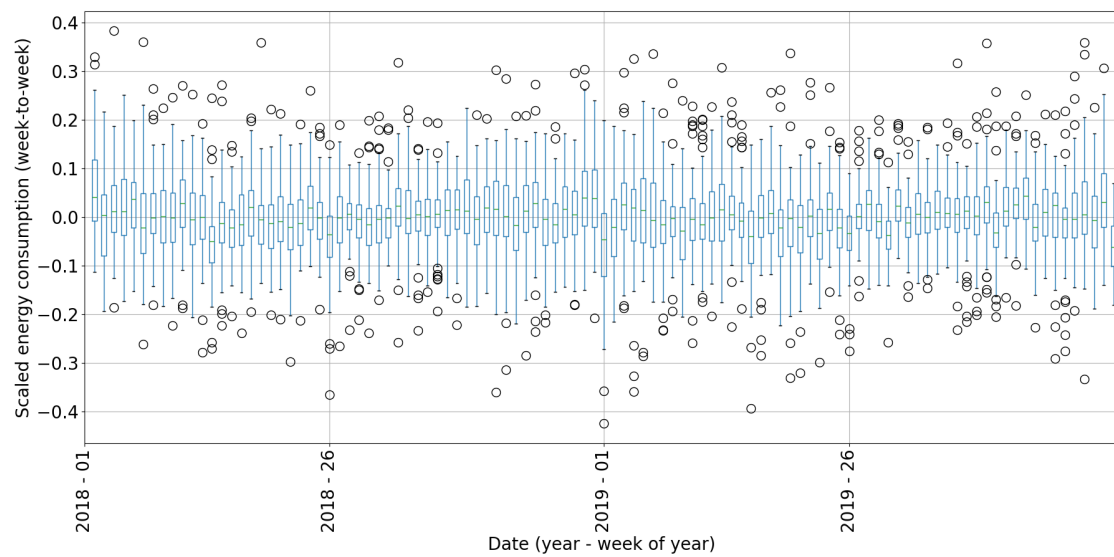


**Figure 6.** Boxplot showing distributions of differential time series for every week of year in the dataset.

Another requirement involves handling non-iid data across multiple clients, which can be simply demonstrated by illustrating correlations among all generated RECTS. Figure 7 shows their correlation matrix  $X_{rec,corr}$ , with highest correlations on the diagonal - representing correlations of each RECTS to itself. Since each REC is individually developed using diverse  $\vec{r}_t$  at start and end point, correlations are much lower than the ones of DECTS (compare Table 1 with Table 3). This strongly indicates, that RECTS possess a high degree of non-iid data, which must be adequately considered within a time series forecasting model and FL.

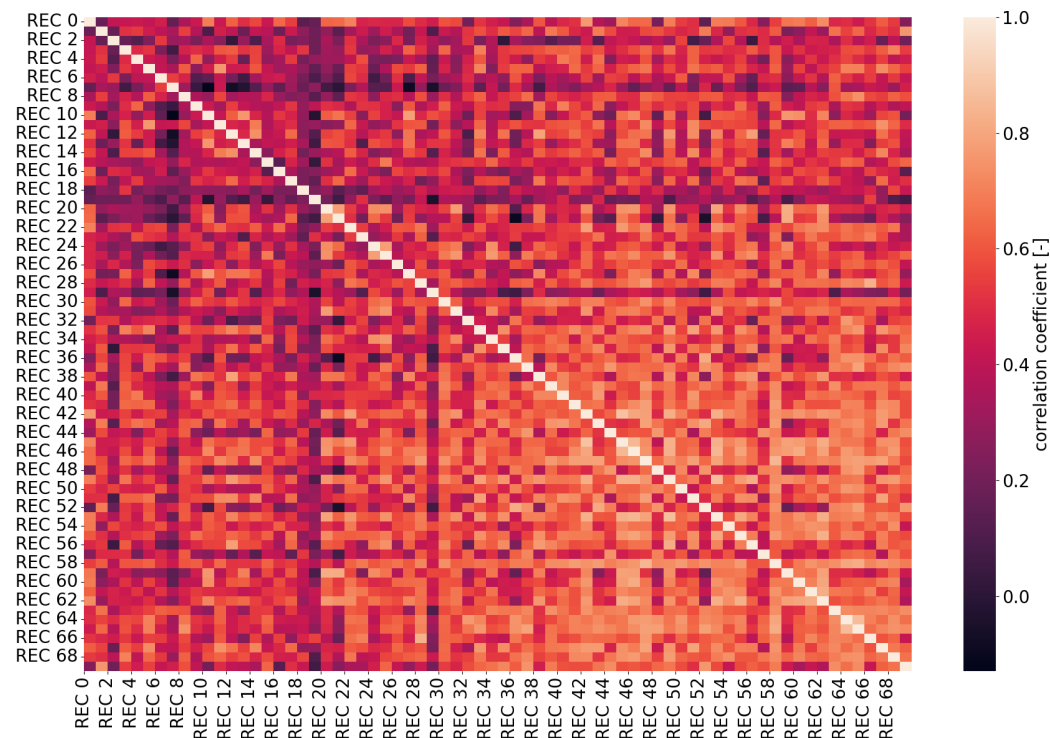


**Figure 7.** Heatmap of correlation matrix  $X_{rec,corr}$  using RECTS as input.

**Table 3.** Statistics of the correlation matrix  $X_{rec,corr}$  for all RECTS.

$\mu(X_{rec,corr})$	$\sigma(X_{rec,corr})$
0.51	0.18

#### 2.4. Transformation

Time series data should be scaled before being used in machine learning, particularly because of algorithm performance and gradient descent optimization. In our work, we utilize Eq. (3) to scale data within the range  $[-1, 1]$  by setting  $a = -1$  and  $b = 1$ . To rescale transformed data to its original magnitude, we use Eq. (4)

$$x' = a + \frac{(x - \min(x)) \times (b - a)}{\max(x) - \min(x)} \quad (3)$$

$$x = \min(x) + \frac{x' \times (\max(x) - \min(x)) - a}{b - a} \quad (4)$$

### 3. Methodology

#### 3.1. Problem Description

Time series are governed by a stochastic process, meaning that both past observations  $X_t$  and random shocks  $\epsilon_t$  directly influence future values  $Y_{t+1}$ . In terms of RECTS, the impact of autoregressive variables  $X_t$  and  $\epsilon_t$  on  $Y_t$  is dependent on temporal features like weekday or daytime and additionally varies from one RECTS to the next, resulting in individual forecast model parameters. The primary challenge is to create a forecast model that learns features which are consistent across different REC residents composition  $\vec{r}_t$  (domains) and can be generalized to a vast array of RECs, even those not included in model training. Moreover, this forecast model should account for non-stationarity and discontinuity with regard to dynamic portfolios of RECs. Since all RECTS are assumed to be located on distributed clients, the model training process must address privacy and security concerns through the application of FL, which must manage non-iid data and weight divergence.

#### 3.2. Concept

Based on the problem description, we develop an approach that satisfies requirements and addresses unresolved challenges. Firstly, we provide a brief description of the time series process of RECTS by illustrating process equations. In addition to exogenous variables such as weather, we precisely incorporate the time-dependent residents composition  $\vec{r}_t$  of RECs into these equations (Section 3.3). Since these process equations reflect past, present, and future states, each with potentially different  $\vec{r}_t$ , we take this into account during the development of the forecast model - feedforward neural network (FNN) (Section 3.4). To train across multiple distributed clients, we also develop a FL framework that offers flexibility in forecast model parameterization (such as layer type, number of neurons, batch size, and optimizer type for gradient descent) and data sharing, aiming to overcome non-iid and model weight divergence issues (Section 3.5). Finally, we set up meaningful experiments to distinguish between ineffective and effective settings (Section 3.6). For this, we must make some assumptions:

- All RECs are composed of the same distinct DECTS, as described in Section 2.2.
- All RECs are aware of the history of their  $\vec{r}_t$ .
- For effective model training using FL, all RECs must share the minimum and maximum values of their RECTS to achieve consistent data scaling over all clients.

#### 3.3. Time Series Process

RECTS, and time series in general, are composed of seasonal (regular long-term or annual variation), periodic (regular short-term or weekday variation), trend (long-term directional movement)

and irregular (white noise, which can not be modeled) components. Time series can be predicted by extrapolating from past and present observations into the future, commonly utilizing an AutoRegressive Integrated with exogenous variables (ARIX) model. In this context, AR is associated with present observations, I is associated with past observations, and X encompasses the impact of exogenous variables across past, present, and possible future (F) events. Then, a time series forecasting model should learn relationships between all variables (endogenous and exogenous) at past, present, and future timestamps. Within this framework, exogenous further variables include data of calendar, weather, and residents composition of REC  $\vec{r}_t$  (Table 4). In our approach, we encode calendar features using cyclical encodings (Definition 13), resulting in lower dimensions [30,31]. We determine the number of lagged values  $p = 2$  that have a strong impact on subsequent values by following the Box-Jenkins method and utilizing the partial autocorrelation function [32]. Since I is utilized to address short-term non-stationarities, we use reference values based on the type of day (such as day of the week, holiday, or bridge day), resulting in the following shifts  $\tau$  (Figure 8):

- monday  $\rightarrow$  last friday ( $\tau = 3days$ )
- tuesday  $\rightarrow$  yesterday ( $\tau = 1days$ )
- wednesday  $\rightarrow$  yesterday ( $\tau = 1days$ )
- thursday  $\rightarrow$  yesterday ( $\tau = 1days$ )
- friday  $\rightarrow$  yesterday ( $\tau = 1days$ )
- saturday  $\rightarrow$  last saturday ( $\tau = 7days$ )
- sunday  $\rightarrow$  last sunday ( $\tau = 7days$ )
- holiday  $\rightarrow$  last sunday ( $\tau = x days$ )
- bridge day  $\rightarrow$  last saturday ( $\tau = x days$ )

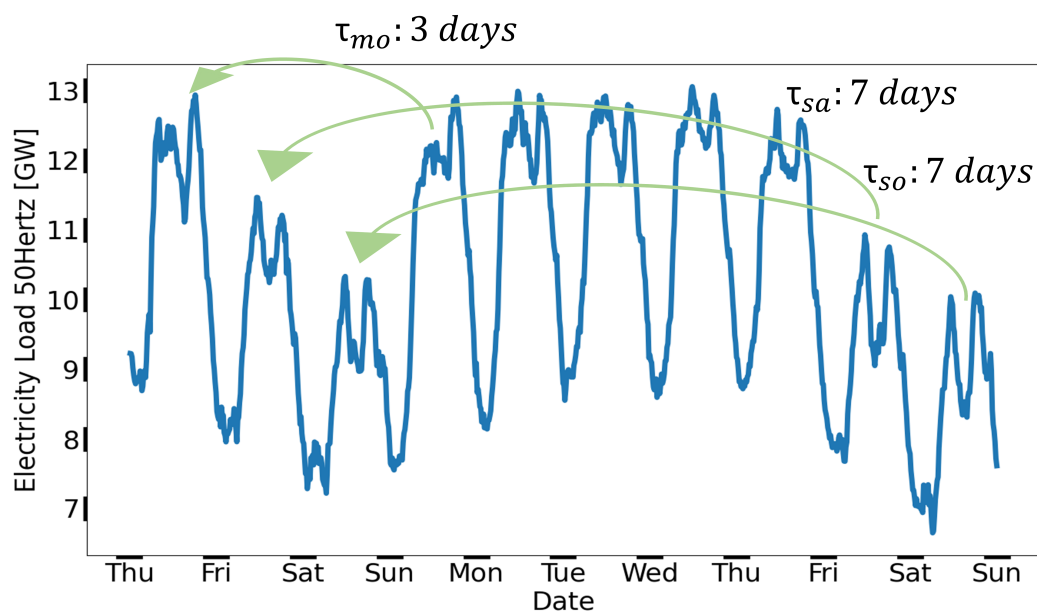


**Figure 8.** Electricity load time series of 50Hertz [36] showing exemplary temporal shifts ( $\tau_{sa}$ : 7 days,  $\tau_{so}$ : 7 days, and  $\tau_{mo}$ : 3 days) used in the integrated part I (Eq. (6)).

With this information, we can formulate regression equations for AR (Eq. (5)), I (Eq. (6)), and F (Eq. (7)) within the context of an ARIX model to generate input data ( $X_{AR}$ ,  $X_I$ ,  $X_F$ ) for the purpose of model training purposes, while disregarding the difference filter. This subsequently yields the complete ARIX process equation (Eq. (8)). Given that historical data of  $\vec{r}_t$  is available for each REC and is also included in the input data, there is potential to extract cross-domain and domain-invariant features, a process known as domain adaptation [33–35].

**Definition 12** (One-Hot Encoding, taken from [15]).

Within a one-hot encoding, each class is represented by a binary vector. In this encoding, each class occurrence assigns to 1 and otherwise to 0.

**Definition 13** (Cyclical Encoding, inspired by [15]).

Periodic encodings are transformations of one-hot encodings into more continuous variables by using sine and cosine functions. This can only be applied to periodic variables like daytime, day of the week or day of the year.

Example: For the cyclical transformation of all hours  $h \in [1, 24]$ , we use both sinus  $\sin\left(\frac{2 \times \pi \times h}{\max(h)}\right)$  and cosine  $\cos\left(\frac{2 \times \pi \times h}{\max(h)}\right)$  transformations to create two new variables.

**Table 4.** Description of endogenous and exogenous variables used in past (I), present (AR) and future (F) regression equations.

data type	variable	description	considered in
target	RECTS	provide target states	AR, I
calendar	day of year (doy)	models annual seasonality	AR, I, F
calendar	day of week (dow)	models short-term periodicity	AR, I, F
calendar	daytime (dt)	models intraday periodicity	AR, I, F
weather	temperature (T)	models T dependencies	AR, I, F
weather	relative humidity (RH)	models RH dependencies	AR, I, F
residents composition	$\vec{r}_t$	models $\vec{r}_t$ dependencies on RECTS stochasticity	AR, I, F

$$X_{AR}(t) = \sum_{j=1}^n \sum_{i=1}^p (\alpha_{j,i} \times x_j(t-i)) \quad (5)$$

$$X_I(t) = \sum_{j=1}^n (\beta_j \times x_j(t-\tau)) \quad (6)$$

$$X_F(t) = \sum_{j=1}^n (\gamma_j \times x_j(t)) \quad (7)$$

$$y(t) = X_{AR} + X_I + X_F \quad (8)$$

where:

- $p$  Number of past observations to be considered in AR
- $\alpha, \beta, \gamma$  Regression parameters within an ARIX model
- $n$  Number of variables used in regression equation (Table 4)
- $x$  variable

### 3.4. Time Series Forecast Model

In the context of time series forecasting, a huge amount of various neural network architectures have been studied [16,31]. While neural networks and ARIX regression models may utilize identical input data (refer to Section 3.3), neural networks do not necessitate a predefined regression equation and are adept at discovering non-linear relationships and latent characteristics. This paper posits that the accuracy of forecasts is largely influenced by the choice of input features, the engineering of features (such as calendar data), and the manner in which past, present and future features are connected within the model's architecture. A time series forecasting model is expected to discern the linkages between past, present and present endogenous and exogenous variables (see Eq. (6), (5)) and leverage this knowledge alongside future exogenous variables (Eq. (7)) to predict the target variable. To this end, we propose a neural network with distinct input layers  $L1_I, L1_{AR}, L1_F$  processing past  $X_I$ , present  $X_{AR}$ , and future  $X_F$  data, each equipped with an equivalent neuron count to facilitate

feature learning. Subsequent to this, latent features are combined following a principle of action (either concatenation or multiplication), and the resulting array is then processed within an output layer  $L2$ , conforming to the target output dimensions (illustrated in Figure 9). This architectural design can be implemented utilizing Dense-layers (FNN). In our work, we use three input layers, each with 30 neurons, and one output layer, with each layer equipped with a linear activation function.

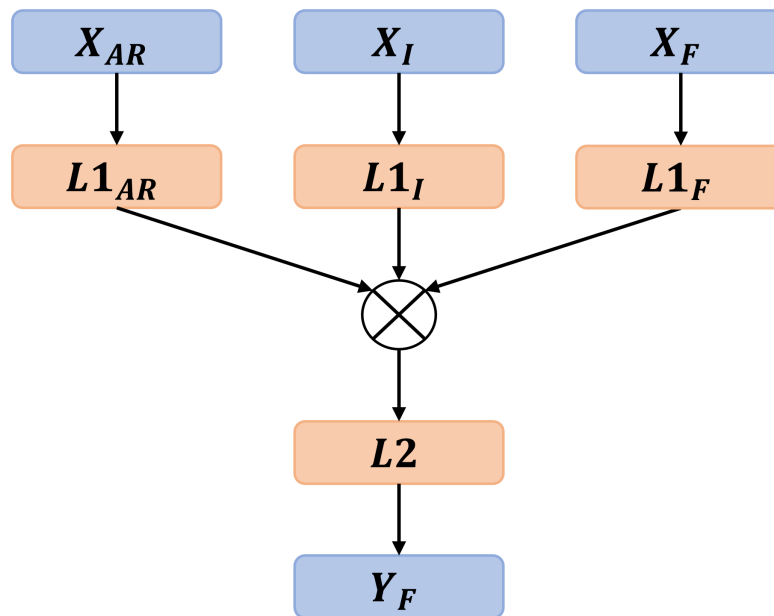


**Figure 9.** Principle neural network architecture with three input-layers  $L1_{AR}$ ,  $L1_I$ ,  $L1_F$  to handle past  $X_I$ , present  $X_{AR}$  and future  $X_F$  data separately and to fit future values of the target variable  $Y_F$ .

### 3.5. Federated Learning

FL was introduced to train a high-quality global model while keeping training data distributed across multiple clients, thereby ensuring data privacy as well as security issues, and demonstrating robustness to non-iid data. Additionally, model performance can be improved by training a model with a diverse array of training data. To achieve this, the FederatedAveraging algorithm (Algorithm 2) applies stochastic gradient descent within local model training and averages each client's model weights on a central server [37]. In the context of energy time series forecasting, many publications have studied the application of FL at household level. Given that this data is highly stochastic and non-iid, they propose using a one-step-ahead forecast horizon and clustering similar clients into groups, resulting in multiple global forecast models, which are further fine-tuned by applying transfer learning [24,25,38–41]. While this approach overcomes issues with non-iid data, there is no one that attempts to unify heterogeneous time series data into a single global forecast model, addressing non-stationarity and discontinuity. The reason for doing so is that a non-iid data setting across multiple clients can lead to a divergence in model weights (Figure 10). Moreover, the number of hidden neurons  $N$  can significantly impact model convergence because gradients tend to increase when  $N$  is low. This effect can be observed during the optimization of model weights that do not align well with local data distributions and characteristics. A common practice, among others, for addressing this effect is to share data across multiple clients, which is beneficial for aggregating knowledge of relational behavior [42] (Figure 11).

**Algorithm 2:** FederatedAveraging

---

```

46 #Training
47 Server initializes forecast model weights  $w_{t=0}$  and sends them to all clients
48 for  $i \leftarrow 1$  to  $N$  (number of FL epochs) by 1 do
49   for  $j \leftarrow 1$  to  $K$  (number of clients) by 1 do
50      $Client_j$  trains forecast model weights  $w_{t=i}^j$  and sends them back to server
51   Server updates models weights to  $w_{t=i}$  using WeightAveraging( $w_t$ ) and sends them back to all
     clients
52
53 WeightAveraging( $w_t$ )
54  $w_{t+1} \leftarrow \sum_{k=1}^K \frac{n_k}{n} w_{t+1}^k$ ; where  $n_k$  and  $n$  equals number of client- and all-samples

```

---

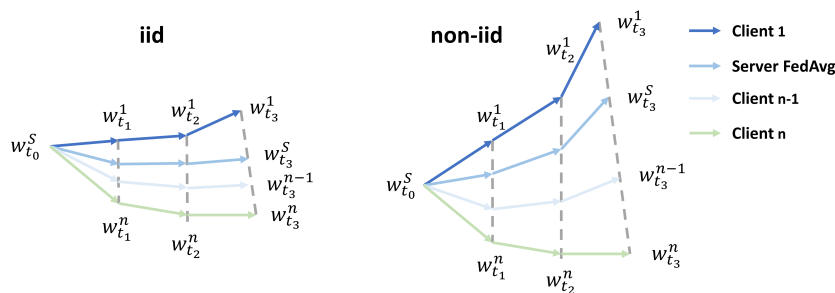


**Figure 10.** The evolution of model weights across local training epochs  $t_0, t_1, t_2, t_3$ , under both independent and identically distributed (iid) and non-iid data scenarios, demonstrates diverging weight patterns (inspired by [43]).

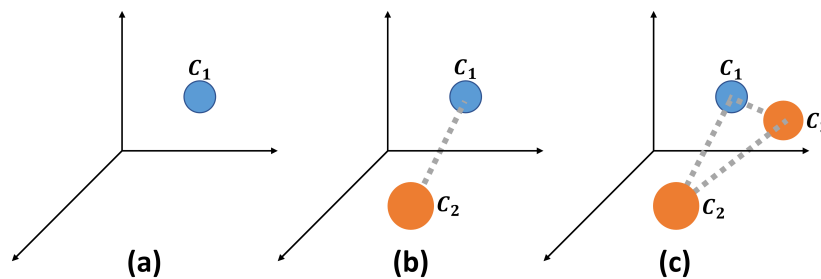


**Figure 11.** Approaches to data sharing include: (a) not sharing any time series, (b) sharing one time series, and (c) sharing two time series.

### 3.6. Experiments

Our work aims to bridge the research gap in training time series forecasting models using Federated Learning, addressing non-stationarity and discontinuity, as previously mentioned in Section 1.4. For this purpose, we outline the time series process, including preprocessing of model input data (Section 3.3), develop a generic neural network architecture that handles non-stationarities, discontinuities, and domain-specific characteristics across various observation times - including past, present, and future (Section 3.4), and construct a FL framework to aggregate knowledge from a diverse set of clients by applying data sharing (Section 3.5). In our experiments, we apply various model parameterizations (Table 5) that include different values for the number of shared time series to each client (sts  $\rightarrow$  extract relational behavior of RECTS with various  $\vec{r}_t$  [42]), the batch size (bs  $\rightarrow$  generalize neural network [44]) and the learning rate (lr  $\rightarrow$  regularize model weight divergence [43]), while maintaining the number of hidden neurons  $N = 30$ , local training epochs  $e = 1$  and FL training epochs  $E = 50$ . While training local forecasting models with stochastic gradient descent, we use Federated Averaging (Algorithm 2) to update global model weights within the entire FL process. Training data is prepared for a subset of  $C_1 = 35$  clients with a small member size, considering the year 2018, and it is

processed for a forecast execution time of 06:00 with a horizon spanning an entire day. To demonstrate our framework's capability concerning domain-adaption, transferability, and performance, we need to design meaningful experiments (test data is a subset of  $C_2 = 35$  clients with large member size, considering the year 2019) that differentiate between ineffective and effective settings (Table 6). Figure 12 illustrates the process of conducting the various experiments. In Appendix C, Figure A2 illustrates the average number of members for each REC and their overall median value  $med$ . Regarding this,  $C_1$  refers to RECs smaller than  $med$  and  $C_2$  refers to RECs larger than  $med$ , dividing train and test dataset into two distinct subsets of time series, each with characteristic behaviors and magnitudes. We use TensorFlow [45], an open-source machine learning framework, and *Stochastic Gradient Descent* optimization algorithm.

**Table 5.** Various forecast model parameterizations in terms of batch size, the number of shared time series to each client, and the learning rate.

Forecast Model	Batch Size $bs$	Shared Time Series $sts$	Learning Rate $lr$
M1	16	0	0.0001
M1	64	0	0.0001
M2	16	2	0.0001
M3	64	2	0.0001
M4	16	0	0.001
M5	64	0	0.001
M6	16	2	0.001
M7	64	2	0.001

**Table 6.** Experiments to be conducted, evaluated, and compared to gain knowledge about effective FL settings for non-stationary, discontinuous, and non-iid RECTS.

No.	Objective	Setting
I.	Train FNN for all RECs regarding $\bar{r}_t$ using federated learning (multi RECTS). In this study, we use $C = 35$ REC with a small member size to illustrate the model's transferability to out-of-sample data.	<ul style="list-style-type: none"> <li>• share RECTS to each client <math>sts \in [0, 2]</math></li> <li>• use multiple batch sizes <math>bs \in [16, 64]</math></li> <li>• use multiple learning rates <math>lr \in [0.001, 0.0001]</math></li> </ul>
II.	Train FNN for each REC neglecting $\bar{r}_t$ (single RECTS) and compare them	<ul style="list-style-type: none"> <li>• Use best setting of experiment I.</li> </ul>
III.	Train FNN for each REC providing $\bar{r}_t$ (single RECTS) and compare them	<ul style="list-style-type: none"> <li>• Use best setting of experiment I.</li> </ul>
IV.	Train a FNN for all RECs neglecting $\bar{r}_t$ (multi RECTS) and compare them	<ul style="list-style-type: none"> <li>• Use best setting of experiment I.</li> </ul>
V.	Train a FNN for all RECs providing $\bar{r}_t$ (multi RECTS) and compare them	<ul style="list-style-type: none"> <li>• Use best setting of experiment I.</li> </ul>

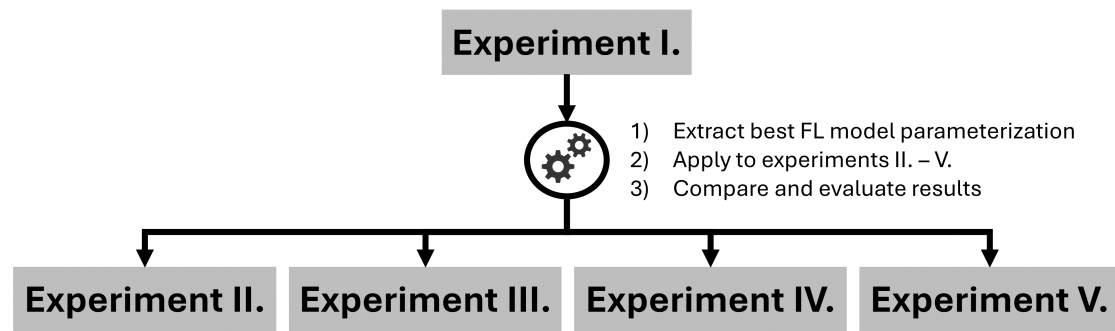


**Figure 12.** Illustration of the process of conducting various experiments: 1) Conduct various FL runs within experiment I. using different configurations concerning shared time series, batch size, and learning rate, 2) extract best configuration from experiment I. and apply it within experiments II. - V., 3) compare and evaluate results.

## 4. Results

### 4.1. Experiment I.

Experiment I is intended to identify the best model setting, which is then applied in subsequent experiments as well. Table 7 displays the mean absolute error (MAE, see Appendix D Eq. (A1)) and the mean absolute percentage error (MAPE, see Appendix D Eq. (A2)) for each model applied to the test dataset (year 2019), showing strong dependencies on batch size, learning rate, and number of shared time series. The results propose to use a smaller batch size (compare error measurements between M0 and M1, between M2 and M3, between M4 and M5, or between M6 and M7), a higher number of shared RECTS with all clients (compare error measurements between M0 and M2, between M1 and M3, between M4 and M6, or between M5 and M7), and a bigger learning rate (compare error measurements between M0 and M4, between M1 and M5, between M2 and M6, or between M3 and M7). While models with higher learning rates converge faster and yield favorable error measurements, the others struggle to learn meaningful latent features necessary for transferable predictions. Moreover,  $E = 50$  federated learning epochs are sufficient for the models to converge (see Figure 13). Since these error measurements do not provide a clear overview of our forecasting framework's capabilities, we further illustrate the predictions versus actual measurements in Figure 14. The scatter plot (a) shows good agreement, except for some outliers that could possibly be caused by high variability during special events, and the line plot (b) confirms these findings. Since M6 provides best prediction results, we will use this setting within the experiments II. - V..

**Table 7.** MAE and MAPE from various models trained with data from clients with a small member size and tested on clients with a large member size.

	M0	M1	M2	M3	M4	M5	M6	M7
<b>MAE [kW]</b>	5.57	7.30	4.10	5.89	2.68	3.85	2.65	3.18
<b>MAPE [%]</b>	17.18	22.70	12.40	18.23	8.10	12.04	8.03	9.77

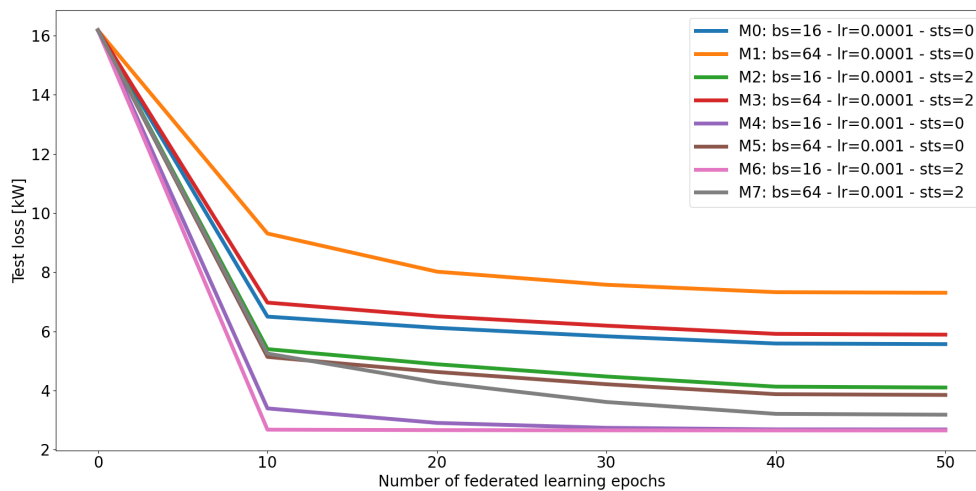


**Figure 13.** Mean absolute error for models M0, M1, M2, M3, M4, M5, M6, M7 applied on test data, depending on the number of federated learning epochs.

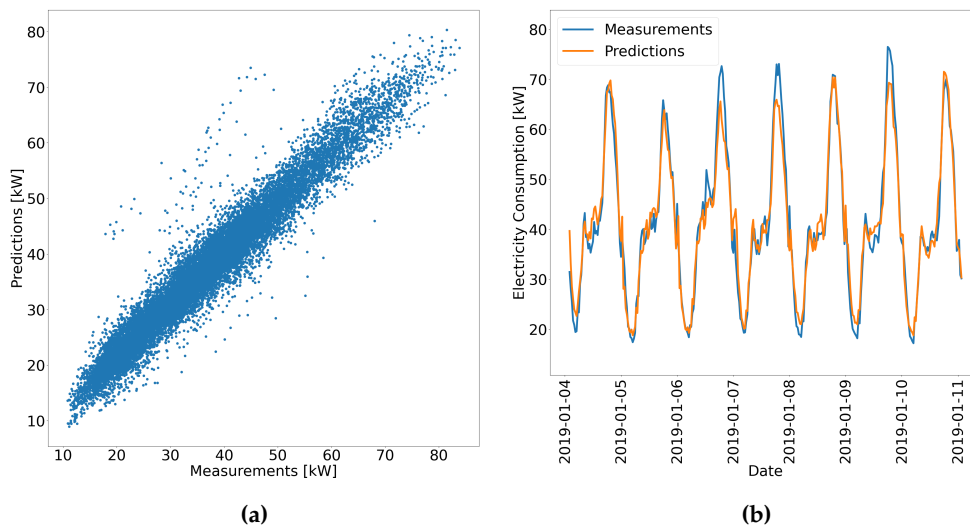


**Figure 14.** Time series forecasts for an exemplary RECTS visualized as a scatter plot (a) and a line plot (b), using the best forecast model M6.

An optimal forecast model is achieved when the error time series (measurements minus predictions) can be proven to be equivalent to white noise [46]. Under such circumstances, the precision of the forecast is at its peak and further refinement is not possible, regardless of additional efforts. Since the partial autocorrelation is the correlation between a time series and its lagged version, excluding the influence of intervening lags, it can be used to determine temporal dependencies in the error time series. Figure 15 illustrates this analysis by applying model M6 to forecast an exemplary RECTS for the year 2019 and using the 12:00 values of the error time series. It is observed that only the partial correlation at lag 0 is significant, indicating a strong self-correlation without temporal dependencies. This measurement can be used to test for white noise in the error time series, indicating no remaining information.

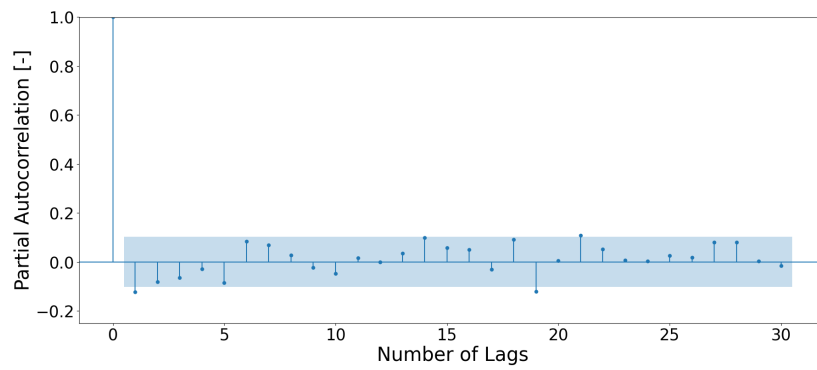


**Figure 15.** Partial autocorrelation of the error series at time 12:00 analyzed using the Python statsmodels package.

#### 4.2. Experiment II.

This experiment uses the best model setting, M6 (Table 5, Section 4.1), trains a single forecast model for each REC using training data from the year 2018 and applies each one to the test data from the year 2019. Since forecast models are usually trained on single client without using auxiliary information like  $\vec{r}_t$ , this procedure can be seen as a very good baseline for comparison. In particular, this analysis can determine the impact that including  $\vec{r}_t$  and various RECs in the model input data has on forecast accuracy, specifically in terms of non-stationary and discontinuous time series. The results in Table 8 show that forecast model performance greatly benefits from using  $\vec{r}_t$  and a big amount of data during model training (federated learned forecast model - FL Model), while neglecting this leads to a significantly larger forecast error (single time series forecast model - Single Model). Moreover, Figure 16 illustrates the distribution of MAE over multiple RECs with large member sizes for both, FL Model and Single Model. Regarding that training and test data are highly non-iid, only the FL Model is particularly capable of handling this circumstance. The reason for this is that the Single Model severely overfits to seasonality by considering day in the model input data without taking the effect of  $\vec{r}_t$  into account. This evaluation demonstrates the importance of model input data and the quantity of training data, and illustrates the capability of our framework to aggregate knowledge from different clients to improve forecast accuracy of RECTS.

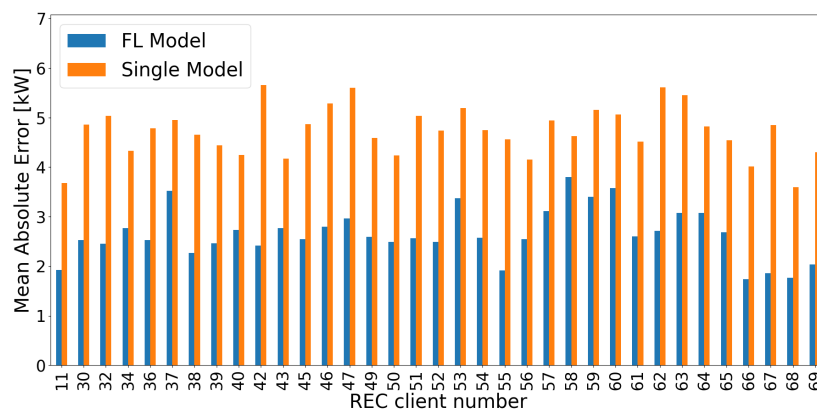


**Figure 16.** MAE of forecast models referred to individual RECs neglecting  $\vec{r}_t$  (orange - Single Model) compared to the best FL model M6 (blue - FL Model) from Section 4.1.

**Table 8.** Means  $\mu$  and standard deviations  $\sigma$  of the errors from forecast models trained on individual RECs neglecting  $\vec{r}_t$  (orange - Single Model) and best forecast model M6 trained on multiple RECs in a federated manner (Table 5, blue - FL Model).

	MAE- $\mu$	MAE- $\sigma$
FL Model	2.65	0.5
Single Model	4.72	0.5

#### 4.3. Experiment III

After Section 4.2 demonstrates bad forecast performances using Single Model, this experiment includes  $\vec{r}_t$  as auxiliary information in the model input data to determine if it can benefit from it. Compared to Tables 8 and 9, this does not confirm this assumption, as the forecast error, in terms of MAE, increases from 4.72 kW to 5.81 kW. Figure 17 visually demonstrates this measurement, indicating a higher magnitude and higher variability of forecast errors. While the Single Model without  $\vec{r}_t$  strongly overfits to the seasonality within the training dataset, the one considering  $\vec{r}_t$  attempts to handle both, seasonality with regards to  $\vec{r}_t$ . Since this further increases the complexity of data processing within the forecast model without providing a variety of samples for specific seasonalities and  $\vec{r}_t$ , forecast accuracy even worsens. A reason for this is the dynamic evolution of  $\vec{r}_t$  (Section 2.2), whose impact on electricity consumption has not been adequately learned in model training due to a lack of data variety. This evaluation further shows that training a forecast model for each individual RECS, whether using  $\vec{r}_t$  or not, is unable to extract domain-invariant features as well as cross-domain behaviors in the context of non-stationary and discontinuous time series. Consequently, both Single Models are not transferable to unseen data. These results confirm that aggregating and extracting relational knowledge from a vast array of diverse data sources is essential to improve forecast accuracy of RECS.

**Table 9.** Means  $\mu$  and standard deviations  $\sigma$  of the errors from forecast models trained on individual RECs taking  $\vec{r}_t$  into account (Single Model) and best forecast model M6 trained on multiple RECs in a federated manner (Table 5, FL Model).

	MAE- $\mu$	MAE- $\sigma$
FL Model	2.65	0.5
Single Model	5.81	1.22

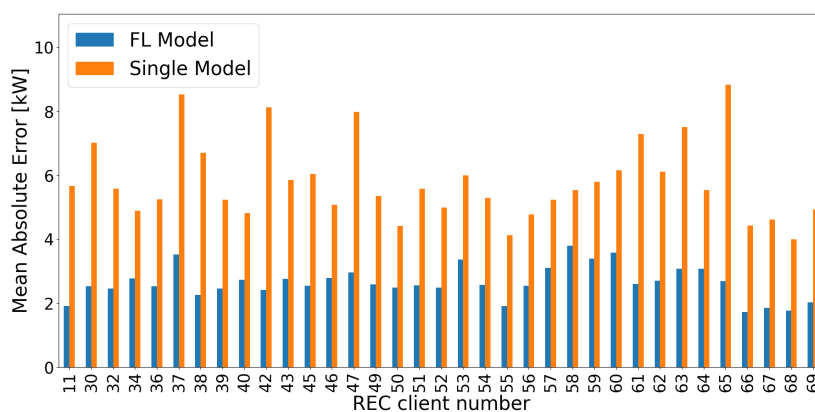


**Figure 17.** MAE of forecast models referred to individual RECs taking  $\vec{r}_t$  into account (orange - Single Model) compared to the best FL model M6 (blue - FL Model) from Section 4.1.

#### 4.4. Experiment IV.

While Section 4.2 and 4.3 aim to compare forecast models trained on single data sources with those trained on multiple sources, Experiment IV evaluates forecast accuracies of a centrally learned forecast model (CL Model) against the best FL Model M6 (Section 4.1) using identical data samples. In this case, the CL Model neglects  $\vec{r}_t$  to obtain a baseline accuracy measurement for a forecast model,

following common ARIX process equations. Table 10 shows a strong improvement compared to Single Models (Tables 8 and 9), but it still does not perform as well as the best FL Model M6 (Section 4.1). Although FL Model is trained in a federated manner, it outperforms CL Model by over 18% in terms of MAE. This strongly suggests the usage of auxiliary data to forecast non-stationary and discontinuous RECTS - Figure 18 demonstrates this behavior for every REC. This evaluation once again shows that FL Model can extract domain-invariant features and cross-domain behaviors by utilizing  $\vec{r}_t$ , resulting in higher forecast accuracies compared to conventional forecast models.

**Table 10.** Means  $\mu$  and standard deviations  $\sigma$  of the errors from forecast models trained centrally on multiple RECs neglecting  $\vec{r}_t$  (CL Model) and best forecast model M6 trained on multiple RECs in a federated manner (Table 5, FL Model).

	MAE- $\mu$	MAE- $\sigma$
FL Model	2.65	0.5
CL Model	3.23	0.48

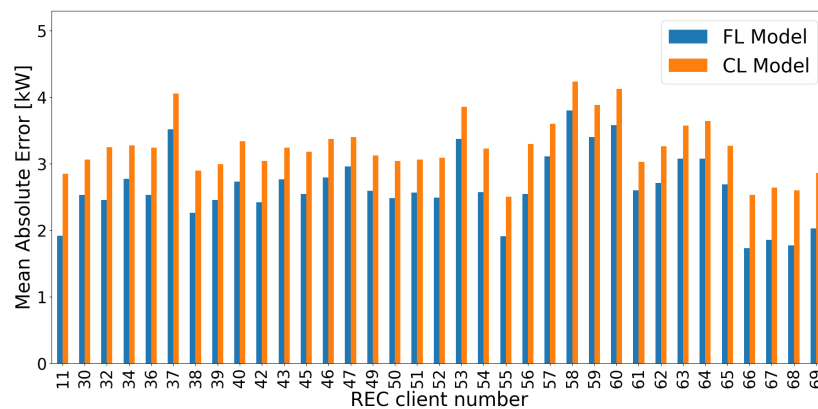


**Figure 18.** MAE of a centralized learned forecast model neglecting  $\vec{r}_t$  (orange - CL Model) compared to the best FL model M6 (blue - FL Model) from Section 4.1.

#### 4.5. Experiment V.

This section is intended to compare CL Model with FL Model using same training and testing samples, as well as same settings outlined in Section 4.1. While Table 11 shows slightly better results for FL Model, Figure 19 illustrates no significant differences in error measurements. These results strongly prove the capability of our framework to forecast non-stationary and discontinuous RECTS, when training a forecast model by applying FL. Moreover, it is able to extract domain-invariant features and cross-domain behaviors as good as a central learned model.

**Table 11.** Means  $\mu$  and standard deviations  $\sigma$  of the errors from forecast models trained centrally on multiple RECs taking  $\vec{r}_t$  into account (CL Model) and best forecast model M6 trained on multiple RECs in a federated manner (Table 5, FL Model).

	MAE- $\mu$	MAE- $\sigma$
FL Model	2.65	0.5
CL Model	2.86	0.43

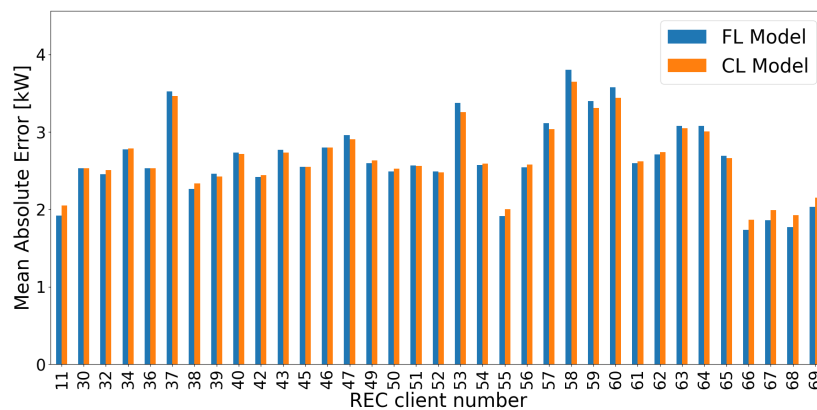


**Figure 19.** MAE of a centralized learned forecast model taking  $\bar{r}_t$  into account (orange - CL Model) compared to the best FL model M6 (blue - FL Model) from Section 4.1.

## 5. Discussion

This work introduces the European energy market, with a particular emphasis on dynamic portfolios of RECs, which have the potential to introduce new business models, enhance energy efficiency, and reduce electricity costs for their members. Besides fostering energy sharing (tenant electricity, electric vehicle charging, etc.), dynamic portfolios also contain risks concerning energy management tasks, e.g., forecasting energy demand or optimizing the energy system including demand side management, which could lead to financial losses, stress on the grid, operational inefficiencies, and member dissatisfaction. The goal of this work is to develop a forecast framework that overcomes non-stationary, discontinuous, and non-iid time series.

Since no real data is available, we synthesize RECTS by initially creating numerous district time series with diverse characteristics and subsequently aggregating them time-dependently. Given only this type of data, we can only simulate the forecasting of RECTS approximately. Various analyses confirm that the generated time series are non-stationary, discontinuous, and non-iid, as these attributes are prerequisites of the research question. Daily portfolio changes may appear extreme, but they can occur if there is a company whose business model involves automatically optimizing portfolios based on the day of the week, accounting for varying patterns of electricity consumption and generation.

To create model input arrays, we refer closely to ARIX time series processing equations, omitting the differencing filter, as neural networks are capable of automatically extracting this feature. Since the composition of residents in RECs might change daily, we divide these arrays into past, present, and future ones. Thereby, we clearly describe the engineering of calendar data to include temporal dependencies of RECTS. To determine the effect of residents composition on RECTS characteristics, we assume that we possess this information for all RECs and days. While such information does not actually exist, we must first label each member time series within a REC by using a sophisticated classification algorithm.

We then develop a forecasting model based on a FNN architecture with three input layers, each taking into account a separate input array representing a specific time interval within the time series process. As each layer extracts latent features across various time horizons, the forecasting model is capable of handling dynamic portfolios. As our primary objective is to analyze the feasibility of a forecasting model trained using FL, we omit considerations of other neural network architectures, such as sequence-to-sequence networks or temporal convolutional networks which might result in better forecast accuracies. Furthermore, we omit hyperparameter optimization regarding the activation function, the number of neurons, and the number of hidden layers to identify optimal settings.

To train a forecasting model across multiple clients with FL, we employ Federated Averaging exclusively for updating model weights, and use stochastic gradient descent for local model training. Additionally, we apply only one training epoch on each client and experiment with various configurations regarding data sharing, batch size, and learning rate to mitigate weight divergence issues.

In contrast, we did not consider techniques such as FedProx [47] and FedDyn [48] that involve the regularization of model weight updates, learning rate degradation [48,49], layer-wise training [50], and a varying quantity of training data samples [49]. Since model convergence strongly depends on the interaction between sample size, batch size, and learning rate, this issue was analyzed and by a more in-depth optimization, there could be significant potential for improvement in model convergence and performance.

Additionally, we perform multiple training sessions of the forecasting model using FL, taking into account various configurations related to the number of shared time series, the learning rate, and the batch size in order to determine the best setting. This one is subsequently applied in similar experiments to demonstrate the effectiveness of our framework, showing that the FL Model and the CL Model have nearly identical performance. Hence, our framework is capable of aggregating knowledge from multiple clients, learning domain-invariant features, and extracting cross-domain behaviors through the application of FL. Moreover, it is transferable to new unseen data. Nevertheless, more sensitivity studies on hyperparameter tuning must be conducted, e.g., testing the required quantity of RECTS to extract the relational knowledge necessary to cause failure, and the application in a real-world scenario should be analyzed. Since the number of RECs could potentially increase significantly, there could be advantages in using FL regarding training time.

## 6. Conclusion

This work examines various forecasting strategies to handle non-stationary, discontinuous, and non-iid time series across distributed clients. After generating a sufficient number of electricity consumption time series for Renewable Energy Communities with dynamic customer portfolios, several data pre-processing methods are tested in conjunction with differently configured forecast model training on either single or multiple time series. Our novel forecasting framework demonstrates the effectiveness of data sharing to learn domain-invariant features and cross-domain behaviors by aggregating knowledge from various data sources using federated learning. Besides ensuring transferability to unseen data, the forecast accuracy is nearly identical to that of a centrally trained forecasting model. Our novel framework possesses the potential to revolutionize electricity demand forecasting for decentralized energy systems by identifying effective training settings. Future work will investigate the performance of more complex forecasting model architectures, as well as the development of appropriate classification algorithms to generate time series labels that can be used as auxiliary information in the model's input data.

## Appendix A. Dickey Fuller Test For All RECTS

Overall, there are 51 strong non-stationary, 8 medium non-stationary, 6 weak non-stationary, and 5 stationary RECTS (Table A1).

**Table A1.** Dickey fuller test statistics for all RECTS (eliminating seasonality, periodicity and trend): (i) stationary, (ii) weak non-stationary, (iii) medium non-stationary, (iv) strong non-stationary

RECTS	Critical Value	Pvalue	1%	5%	10%
0	-2.61	0.09	-3.44	-2.87	-2.57
1	-1.83	0.37	-3.44	-2.87	-2.57
2	-2.13	0.23	-3.44	-2.87	-2.57
3	-1.93	0.32	-3.44	-2.87	-2.57
4	-2.63	0.09	-3.44	-2.87	-2.57
5	-2.75	0.07	-3.44	-2.87	-2.57
6	-2.15	0.22	-3.44	-2.87	-2.57
7	-4.01	0.0	-3.44	-2.87	-2.57
8	-3.58	0.01	-3.44	-2.87	-2.57
9	-2.71	0.07	-3.44	-2.87	-2.57
10	-3.16	0.02	-3.44	-2.87	-2.57
11	-3.83	0.0	-3.44	-2.87	-2.57
12	-3.46	0.01	-3.44	-2.87	-2.57
13	-2.18	0.21	-3.44	-2.87	-2.57
14	-1.92	0.32	-3.44	-2.87	-2.57
15	-2.51	0.11	-3.44	-2.87	-2.57
16	-2.43	0.13	-3.44	-2.87	-2.57
17	-2.39	0.14	-3.44	-2.87	-2.57
18	-2.96	0.04	-3.44	-2.87	-2.57
19	-2.78	0.06	-3.44	-2.87	-2.57
20	-2.32	0.17	-3.44	-2.87	-2.57
21	-2.11	0.24	-3.44	-2.87	-2.57
22	-2.75	0.07	-3.44	-2.87	-2.57
23	-2.94	0.04	-3.44	-2.87	-2.57
24	-2.19	0.21	-3.44	-2.87	-2.57
25	-2.08	0.25	-3.44	-2.87	-2.57
26	-2.96	0.04	-3.44	-2.87	-2.57
27	-1.91	0.33	-3.44	-2.87	-2.57
28	-2.19	0.21	-3.44	-2.87	-2.57
29	-2.04	0.27	-3.44	-2.87	-2.57
30	-1.87	0.34	-3.44	-2.87	-2.57
31	-2.11	0.24	-3.44	-2.87	-2.57
32	-3.01	0.03	-3.44	-2.87	-2.57
33	-2.48	0.12	-3.44	-2.87	-2.57
34	-1.79	0.38	-3.44	-2.87	-2.57
35	-2.09	0.25	-3.44	-2.87	-2.57
36	-1.61	0.48	-3.44	-2.87	-2.57
37	-1.77	0.39	-3.44	-2.87	-2.57
38	-1.77	0.4	-3.44	-2.87	-2.57
39	-2.15	0.23	-3.44	-2.87	-2.57
40	-1.47	0.55	-3.44	-2.87	-2.57
41	-2.11	0.24	-3.44	-2.87	-2.57
42	-1.43	0.57	-3.44	-2.87	-2.57
43	-1.87	0.34	-3.44	-2.87	-2.57
44	-1.91	0.33	-3.44	-2.87	-2.57
45	-2.01	0.28	-3.44	-2.87	-2.57
46	-2.32	0.16	-3.44	-2.87	-2.57
47	-1.77	0.4	-3.44	-2.87	-2.57
48	-1.69	0.43	-3.44	-2.87	-2.57
49	-2.42	0.14	-3.44	-2.87	-2.57
50	-2.02	0.28	-3.44	-2.87	-2.57
51	-2.7	0.07	-3.44	-2.87	-2.57
52	-2.65	0.08	-3.44	-2.87	-2.57
53	-2.41	0.14	-3.44	-2.87	-2.57
54	-1.92	0.32	-3.44	-2.87	-2.57
55	-1.63	0.47	-3.44	-2.87	-2.57
56	-1.88	0.34	-3.44	-2.87	-2.57
57	-2.35	0.16	-3.44	-2.87	-2.57
58	-2.17	0.22	-3.44	-2.87	-2.57
59	-1.88	0.34	-3.44	-2.87	-2.57
60	-0.85	0.81	-3.44	-2.87	-2.57
61	-1.61	0.48	-3.44	-2.87	-2.57
62	-2.08	0.25	-3.44	-2.87	-2.57
63	-1.87	0.35	-3.44	-2.87	-2.57
64	-1.22	0.66	-3.44	-2.87	-2.57
65	-2.13	0.23	-3.44	-2.87	-2.57
66	-2.14	0.23	-3.44	-2.87	-2.57
67	-2.2	0.2	-3.44	-2.87	-2.57
68	-2.88	0.05	-3.44	-2.87	-2.57
69	-3.49	0.01	-3.44	-2.87	-2.57

## Appendix B. Example Time Series Of Renewable Energy Communities

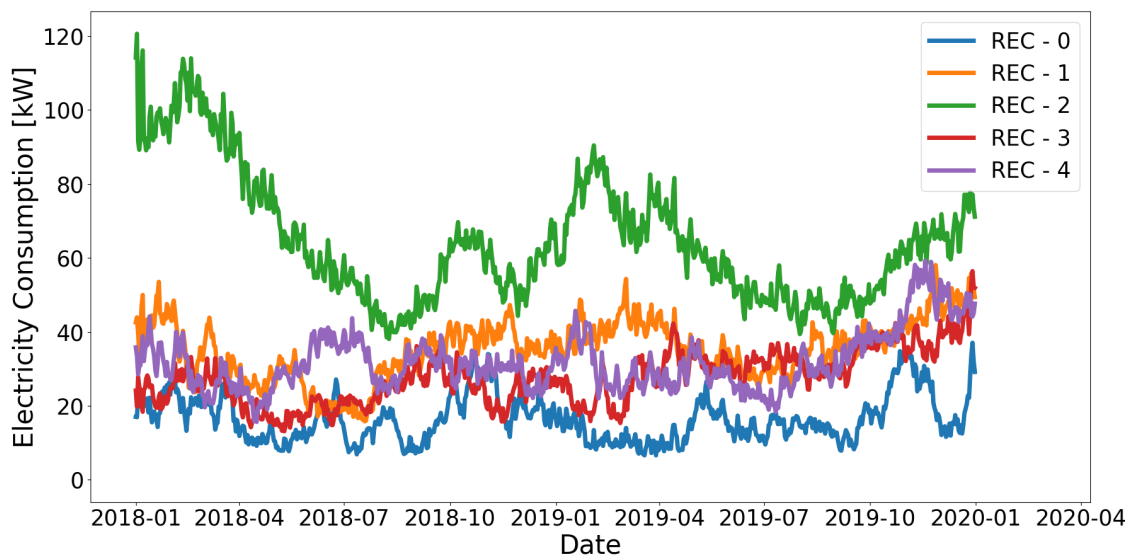


Figure A1. Exemplary RECTS showing non-stationarities.

## Appendix C. Average Member Number Of Renewable Energy Communities

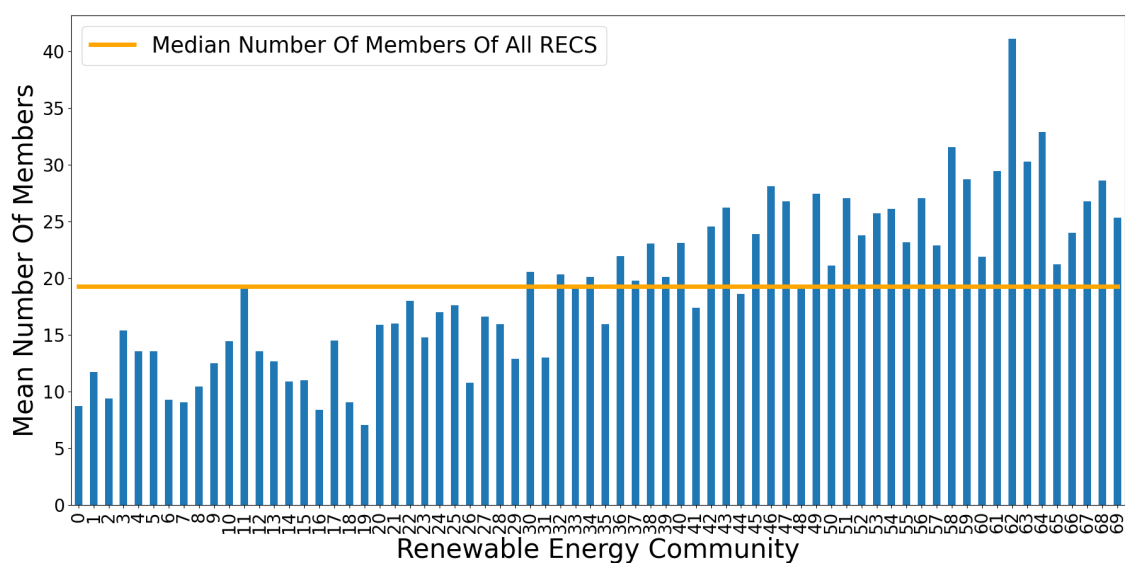


Figure A2. Average size of individual REC members.

## Appendix D. Error Metrics

$$MAE = \frac{1}{n} \sum_{i=1}^n |y_i - \hat{y}_i| \quad (A1)$$

$$MAPE = \frac{1}{n} \sum_{i=1}^n \left| \frac{y_i - \hat{y}_i}{y_i} \right| \quad (A2)$$

where  $y_i$  represents measurements and  $\hat{y}_i$  represents forecasts

## Appendix E. Abbreviations

ADF	Augmented Dickey-Fuller test
AR	AutoRegressive
ARIX	AutoRegressive Integrated with eXogenous variables
bs	Batch size
CL Model	Centrally learned forecast model
DECTS	District electricity consumption time series
DEMS	District energy management systems
F	Future part within ARIMA
FL	Federated learning
FL Model	Federated learned forecast model
FNN	Feedforward neural network
I	Integrated part within ARIMA
IQR	Interquartile range
lr	Learning rate
MAE	Mean absolute error
MAPE	Mean absolute percentage error
ML	Machine learning
non-iid	Non-identical and independently distributed
Q1	First quartile
Q2	Second quartile
Q3	Third quartile
REC	Renewable Energy Communities
RECTS	REC time series
REC-ECF	REC energy consumption forecasting algorithms
REC-EMS	REC energy management systems
RED II	Renewable Energy Directive
Single Model	Single time series forecast model
sts	Shared time series to each client

**Author Contributions:** Conceptualization, L.R.; Methodology, L.R.; Validation, L.R.; Formal analysis, S.L.; Writing—original draft, L.R.; Writing—review & editing, L.R. and S.L.; Visualization, L.R.; Supervision, S.L. and P.B. All authors have read and agreed to the published version of the manuscript.

**Funding:** This research was funded by the Federal Ministry for Economic Affairs and Climate Action in Germany grant number 01MK20013A

**Data Availability Statement:** The raw data supporting the conclusions of this article will be made available by the authors on request.

**Conflicts of Interest:** The authors declare no conflicts of interest.

## References

1. <https://www.ipcc.ch/sr15/chapter/chapter-1/>. visited on 2024-02-07.
2. <https://www.europarl.europa.eu/factsheets/de/sheet/45/energiebinnenmarkt>. visited on 2023-01-05.
3. <https://eur-lex.europa.eu/legal-content/DE/TXT/PDF/?uri=CELEX:02018L2001-20181221&from=EN>. visited on 2023-01-05.
4. [https://www.bmwk.de/Redaktion/DE/Publikationen/Energie/7-energieforschungsprogramm-der-bundesregierung.pdf?\\_\\_blob=publicationFile&v=4](https://www.bmwk.de/Redaktion/DE/Publikationen/Energie/7-energieforschungsprogramm-der-bundesregierung.pdf?__blob=publicationFile&v=4). visited on 2023-01-05.
5. Sauerbrey, J.; Bender, T.; Flemming, S.; Martin, A.; Naumann, S.; Warweg, O. Towards intelligent energy management in energy communities: Introducing the district energy manager and an IT reference architecture for district energy management systems. *Energy Reports* **2024**, *11*, 2255–2265. doi:<https://doi.org/10.1016/j.egy.2024.01.06>
6. Abrahamse, W.; Steg, L. Factors Related to Household Energy Use and Intention to Reduce It: The Role of Psychological and Socio-Demographic Variables. *Human Ecology Review* **2011**, *18*, 30–40.
7. Flemming, S.; Bender, T.; Surmann, A.; Pelka, S.; Martin, A.; Kuehnbach, M. Vor-Ort-Systeme als flexibler Baustein im Energiesystem ? Eine cross-sektorale Potenzialanalyse **2023**. doi:10.24406/publica-897.

8. Beucker, S.; Bergesen, J.; Gibon, T. Building Energy Management Systems: Global Potentials and Environmental Implications of Deployment. *Journal of Industrial Ecology* **2015**, *20*, n/a–n/a. doi:10.1111/jiec.12378.
9. <https://wirtschaftslexikon.gabler.de/definition/energiemanagementsystem-53996>. visited on 2023-01-06.
10. Richter, L.; Lehna, M.; Marchand, S.; Scholz, C.; Dreher, A.; Klaiber, S.; Lenk, S. Artificial Intelligence for Electricity Supply Chain automation. *Renewable and Sustainable Energy Reviews* **2022**, *163*, 112459. doi:https://doi.org/10.1016/j.rser.2022.112459.
11. [https://www.gesetze-im-internet.de/enwg\\_2005/\\_41a.html](https://www.gesetze-im-internet.de/enwg_2005/_41a.html). visited on 2024-02-07.
12. Klaiber, S. Analyse, Identifikation und Prognose preisbeeinflussster elektrischer Lastzeitreihen. PhD thesis, Technische Universität Ilmenau, 2020.
13. <https://eur-lex.europa.eu/legal-content/en/TXT/?uri=CELEX:32019L0944>. visited on 2024-02-07.
14. Hyndman, R.; Athanasopoulos, G. *Forecasting: Principles and Practice*, 2nd ed.; OTexts: Australia, 2018.
15. Richter, L.; Bender, T.; Lenk, S.; Bretschneider, P. Generating Synthetic Electricity Load Time Series at District Scale Using Probabilistic Forecasts. *Energies* **2024**, *17*.
16. Han, Z.; Zhao, J.; Leung, H.; Ma, K.F.; Wang, W. A Review of Deep Learning Models for Time Series Prediction. *IEEE Sensors Journal* **2021**, *21*, 7833–7848. doi:10.1109/JSEN.2019.2923982.
17. Runge, J.; Zmeureanu, R. A Review of Deep Learning Techniques for Forecasting Energy Use in Buildings. *Energies* **2021**, *14*, 608. doi:10.3390/en14030608.
18. Bot, K.; Ruano, A.; Ruano, M., Forecasting Electricity Consumption in Residential Buildings for Home Energy Management Systems; 2020; pp. 313–326. doi:10.1007/978-3-030-50146-4\_24.
19. Wang, W.; Hussain, F.; Lian, Z.; Yin, Z.; Gadekallu, T.; Pham, Q.V.; Dev, K.; Su, C. Secure-Enhanced Federated Learning for AI-Empowered Electric Vehicle Energy Prediction. *IEEE Consumer Electronics Magazine* **2021**. doi:10.1109/MCE.2021.3116917.
20. Lu, Y.; Tian, Z.; Zhou, R.; Liu, W. A general transfer learning-based framework for thermal load prediction in regional energy system. *Energy* **2021**, *217*, 119322. doi:https://doi.org/10.1016/j.energy.2020.119322.
21. Suryanarayana, G.; Lago, J.; Geysen, D.; Aleksiejuk, P.; Johansson, C. Thermal load forecasting in district heating networks using deep learning and advanced feature selection methods. *Energy* **2018**, *157*. doi:10.1016/j.energy.2018.05.111.
22. Shirzadi, N.; Nizami, A.; Khazen, M.; Nik Bakht, M. Medium-Term Regional Electricity Load Forecasting through Machine Learning and Deep Learning. *Designs* **2021**, *5*, 27. doi:10.3390/designs5020027.
23. Liu, H.; Zhang, X.; Shen, X.; Sun, H. A Federated Learning Framework for Smart Grids: Securing Power Traces in Collaborative Learning, 2021. doi:10.48550/ARXIV.2103.11870.
24. Taïk, A.; Cherkaoui, S. Electrical Load Forecasting Using Edge Computing and Federated Learning. ICC 2020 - 2020 IEEE International Conference on Communications (ICC), 2020, pp. 1–6. doi:10.1109/ICC40277.2020.9148937.
25. Gholizadeh, N.; Musilek, P. Federated learning with hyperparameter-based clustering for electrical load forecasting. *Internet of Things* **2021**, *17*, 100470. doi:10.1016/j.iot.2021.100470.
26. <https://www.caci.co.uk/wp-content/uploads/2021/06/Acorn-User-Guide-2020.pdf>. visited on 2024-05-16.
27. Gardner, W.A.; Napolitano, A.; Paura, L. Cyclostationarity: Half a century of research. *Signal Processing* **2006**, *86*, 639–697. doi:https://doi.org/10.1016/j.sigpro.2005.06.016.
28. Aminikhanghahi, S.; Cook, D. A Survey of Methods for Time Series Change Point Detection. *Knowledge and Information Systems* **2017**, *51*. doi:10.1007/s10115-016-0987-z.
29. Schwertman, N.C.; Owens, M.A.; Adnan, R. A simple more general boxplot method for identifying outliers. *Computational Statistics And Data Analysis* **2004**, *47*, 165–174. doi:https://doi.org/10.1016/j.csda.2003.10.012.
30. Pinheiro, M.; Madeira, S.; Francisco, A. Short-term electricity load forecasting - A systematic approach from system level to secondary substations. *Applied Energy* **2023**, *332*, 120493. doi:10.1016/j.apenergy.2022.120493.
31. Gasparin, A.; Lukovic, S.; Alippi, C. Deep Learning for Time Series Forecasting: The Electric Load Case, 2019, [arXiv:cs.LG/1907.09207].
32. Tunnicliffe Wilson, G. *Time Series Analysis: Forecasting and Control*, 5th Edition, by George E. P. Box, Gwilym M. Jenkins, Gregory C. Reinsel and Greta M. Ljung, 2015. Published by John Wiley and Sons Inc., Hoboken, New Jersey, pp. 712. ISBN: 978-1-118-67502-1. *Journal of Time Series Analysis* **2016**, *37*, n/a–n/a. doi:10.1111/jtsa.12194.
33. Shi, Y.; Ying, X.; Yang, J. Deep Unsupervised Domain Adaptation with Time Series Sensor Data: A Survey. *Sensors* **2022**, *22*. doi:10.3390/s22155507.

34. Purushotham, S.; Carvalho, W.; Nilanon, T.; Liu, Y. Variational Recurrent Adversarial Deep Domain Adaptation. 2019.
35. Arik, S.O.; Yoder, N.C.; Pfister, T. Self-Adaptive Forecasting for Improved Deep Learning on Non-Stationary Time-Series, 2022, [arXiv:cs.LG/2202.02403].
36. <https://transparency.entsoe.eu>. visited on 2023-11-28.
37. McMahan, H.B.; Moore, E.; Ramage, D.; Hampson, S.; y Arcas, B.A. Communication-Efficient Learning of Deep Networks from Decentralized Data, 2023, [arXiv:cs.LG/1602.05629].
38. Shi, Y.; Xu, X. Deep Federated Adaptation: An Adaptative Residential Load Forecasting Approach with Federated Learning. *Sensors* **2022**, *22*, 3264. doi:10.3390/s22093264.
39. Wang, Y.; Gao, N.; Hug, G. Personalized Federated Learning for Individual Consumer Load Forecasting. *CSEE Journal of Power and Energy Systems* **2023**, *9*, 326–330. doi:10.17775/CSEEJPES.2021.07350.
40. Chen, J.; Gao, T.; Si, R.; Dai, Y.; Jiang, Y.; Zhang, J. Residential Short Term Load Forecasting Based on Federated Learning. 2022 IEEE 2nd International Conference on Digital Twins and Parallel Intelligence (DTPI), 2022, pp. 1–6. doi:10.1109/DTPI55838.2022.9998969.
41. Savi, M.; Olivadese, F. Short-Term Energy Consumption Forecasting at the Edge: A Federated Learning Approach. *IEEE Access* **2021**, *9*, 1–21. doi:10.1109/ACCESS.2021.3094089.
42. Zhu, H.; Xu, J.; Liu, S.; Jin, Y. Federated Learning on Non-IID Data: A Survey, 2021, [arXiv:cs.LG/2106.06843].
43. Zhao, Y.; Li, M.; Lai, L.; Suda, N.; Civin, D.; Chandra, V. Federated Learning with Non-IID Data **2018**. doi:10.48550/ARXIV.1806.00582.
44. Keskar, N.S.; Mudigere, D.; Nocedal, J.; Smelyanskiy, M.; Tang, P.T.P. On Large-Batch Training for Deep Learning: Generalization Gap and Sharp Minima, 2017, [arXiv:cs.LG/1609.04836].
45. <https://www.tensorflow.org>. visited on 2024-03-13.
46. Schlittgen, R.; Streitberg, B.H. *Zeitreihenanalyse*; Oldenbourg Wissenschaftsverlag, 2001. doi:doi:10.1524/9783486710960.
47. Li, T.; Sahu, A.K.; Zaheer, M.; Sanjabi, M.; Talwalkar, A.; Smith, V. Federated Optimization in Heterogeneous Networks, 2020, [arXiv:cs.LG/1812.06127].
48. Acar, D.A.E.; Zhao, Y.; Navarro, R.M.; Mattina, M.; Whatmough, P.N.; Saligrama, V. Federated Learning Based on Dynamic Regularization, 2021, [arXiv:cs.LG/2111.04263].
49. Li, X.; Huang, K.; Yang, W.; Wang, S.; Zhang, Z. On the Convergence of FedAvg on Non-IID Data, 2020, [arXiv:stat.ML/1907.02189].
50. Charles, Z.; Garrett, Z.; Huo, Z.; Shmulyian, S.; Smith, V. On Large-Cohort Training for Federated Learning, 2021, [arXiv:cs.LG/2106.07820].

**Disclaimer/Publisher's Note:** The statements, opinions and data contained in all publications are solely those of the individual author(s) and contributor(s) and not of MDPI and/or the editor(s). MDPI and/or the editor(s) disclaim responsibility for any injury to people or property resulting from any ideas, methods, instructions or products referred to in the content.